

Observational Constraints on Pulsar Wind Theories

J.G. Kirk

Max-Planck-Institut für Kernphysik, Postfach 10 39 80, 69029 Heidelberg, Germany

`john.kirk@mpi-hd.mpg.de`

ABSTRACT

Two-dimensional, relativistic, MHD simulations of pulsar-wind powered nebulae provide strong constraints on the properties of the winds themselves. In particular, they confirm that Poynting flux must be converted into particle energy close to or inside the termination shock front, emphasising the puzzle known as the σ paradox. To distinguish between the different possible resolutions of this paradox, additional observational constraints are required. In this paper, I briefly discuss two recent developments in this respect: the modelling of high time-resolution optical polarimetry of the Crab pulsar, and the detection of the pulsar/Be star binary PSR 1259-63 in TeV energy gamma-rays.

Subject headings: Stars: pulsars – MHD – Radiation mechanisms

1. Introduction

Our view of the nebulae powered by pulsar winds has matured dramatically in the past few years, largely as a result of high resolution images in the X-ray band (Weisskopf et al. 2000; Gaensler et al. 2001; Helfand et al. 2001; Gaensler et al. 2002; Lu et al. 2002; Gaensler et al. 2003; Pavlov et al. 2003) complemented, in the case of the Crab Nebula, by high resolution optical images (Hester et al. 1995, 2002). This has motivated at least three groups of researchers to perform 2D, relativistic MHD simulations (Komisarov & Lyubarsky 2003, 2004; Del Zanna et al. 2004; Bogovalov et al. 2005). The pulsar wind provides the inner boundary conditions for these simulations, which are concerned with the subsonic flow downstream of the wind's termination shock front. Contact with observation is established by computing the synchrotron emissivity of the flows, assuming injection of relativistic electrons with a prescribed spectrum at the termina-

tion shock. Overall, the observed synchrotron morphology, with its rings, asymmetric torii and jet structures, is fairly convincingly reproduced, although some of the details still evade explanation (Shibata et al. 2003; Mori et al. 2004), and some interesting phenomena demand a kinetic approach (Spitkovsky & Arons 2004). There is a consensus on the requirements these simulations place on the properties of the pulsar wind: the energy flux must be concentrated in the pulsar's equatorial plane, and, at least in the case of the Crab, the fraction of this energy transported as Poynting flux must be small. This fraction is measured by an average over the surface of the shock of the σ parameter, defined as the ratio in the co-moving frame of the magnetic enthalpy density $B^2/4\pi$ to the enthalpy density of the plasma, including its rest-mass. For the Crab Nebula, observations suggest $\sigma \approx 10^{-3}$. This is puzzling, because, on the one hand, standard theories of pair production by pulsars (Daugherty & Hard-

ing 1982; Hirschman & Arons 2001a,b) imply a large value of σ at the point where the wind is launched, and, on the other, because a relativistic, ideal MHD wind does not appear to permit a significant reduction of σ during propagation (Bogovalov 2001). This puzzle is not new (e.g., Kennel & Coroniti 1984), and has been termed the “ σ paradox”, or “ σ problem”

Several resolutions of the paradox have been proposed. It is possible that magnetic collimation may indeed result in the desired conversion, if the initial conditions in the wind are sufficiently anisotropic (Vlahakis 2004). Alternatively, the conversion may take place in a thin layer associated with the termination shock itself (Lyubarsky 2003), or may even be to some extent hidden in the downstream (nebular) flow (Begelman 1998; Shibata et al. 2003).

A hypothesis that has recently received attention is that dissipation within the wind zone causes the conversion. Coroniti (1990) and Michel (1994) originally pointed out that this might happen at the boundary between layers of magnetic field of opposite polarity in the “striped wind”. However, the associated acceleration of the wind causes a significant dilation of the dissipation timescale, an effect omitted in the earlier calculations. Assuming a gradual acceleration process, it is possible to calculate the evolution of the entropy wave that constitutes the stripes in a short wavelength approximation (Lyubarsky & Kirk 2001). Solutions have been found (Kirk & Skjærraasen 2003) in which the Lorentz factor Γ varies as a power of the radius r :

$$\Gamma \propto r^q \text{ with } 1/3 < q < 1/2. \quad (1)$$

The dissipation proceeds fastest in the solution with the slowest acceleration, $\Gamma \propto r^{1/3}$. Complete conversion of magnetic into particle energy before reaching the termination shock was found to be marginally possible in the case of the Crab pulsar wind.

Which, if any, of these possibilities will provide the definitive resolution of the paradox can

only be decided with the help of observational constraints. These are difficult to find. The wind itself, if mostly cold, does not radiate synchrotron radiation and so it is difficult to determine its structure. Recently, however, there have been two observational developments that do appear to hold out the promise of useful constraints.

In the first, high time-resolution optical polarimetry of the Crab pulsar have become available that find a plausible explanation under the hypothesis that the high energy pulses from the Crab pulsar are formed in the pulsar wind. If this interpretation is correct, the high-energy pulsed radiation from this and other pulsars may provide us with a direct view of the conversion process itself.

The second development concerns the detection in TeV gamma-rays of the binary system PSR 1259-63. This offers a diagnostic of the pulsar wind as it enters its termination shock. Because the stand-off distance of the shock from the pulsar varies with binary phase, it may prove possible to extract the dependence of the wind’s Lorentz factor on distance from the pulsar, thus testing the acceleration models.

2. Polarisation of optical pulses from the Crab pulsar

If the hot particles between the stripes of a relativistic, radial wind emit radiation, the effect of Doppler boosting will cause it to appear to the observer to be pulsed, provided that the radius r of the radiating zone satisfies

$$\frac{r}{r_L} < \Gamma^2 \quad (2)$$

where r_L is the radius at which the corotation speed would become luminal and Γ is the bulk Lorentz factor of the wind. This led to the suggestion (Kirk et al. 2002) that the twin-pulse profile observed in the Crab pulsar, as well as in the gamma-ray emission of other pulsars, is a manifestation of the fact that two sections of the current sheet are visible per period in the striped wind

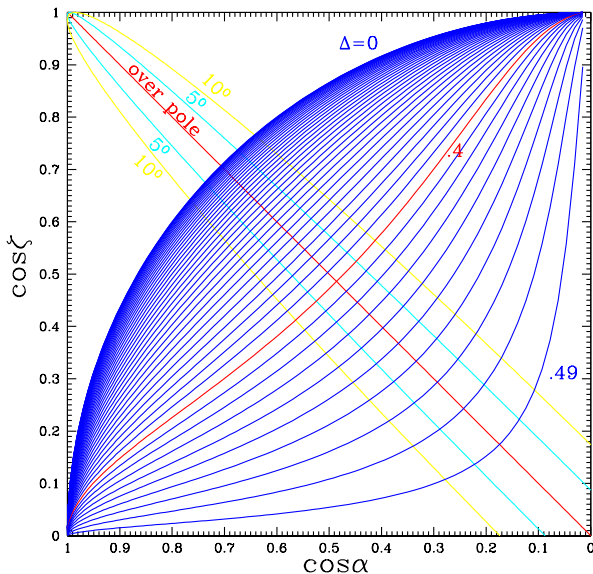


Fig. 1.— The parameter space of pulsar inclination angles ζ (between the rotation axis and the line of sight) and α (between the rotation axis and the magnetic axis). Lines joining the lower left with the upper right corners (blue and red on-line) are contours of constant phase separation Δ of the twin pulses produced in the striped wind model (equally spaced by 0.01 between $\Delta = 0$ and $\Delta = 0.49$). Lines joining the upper left with the lower right corners are lines of equal “impact parameter”, i.e., minimum angle between the line of sight and the magnetic axis. The diagonal (red on-line) corresponds to a line of sight that passes directly over the magnetic pole, the other two pairs to minimum angles of 5° (cyan on-line) and 10° (yellow on-line). The spacing of the Crab pulses, 0.4, corresponds to the labelled contour (red on-line) and the $\zeta \approx 60^\circ$ and $\alpha \approx 60^\circ$ angles favoured by the emission model occur at the intersection of this contour with the “over pole” diagonal.

model. If this interpretation is correct, it constrains the angles ζ between the rotation axis of the pulsar and the line of sight and α , between the magnetic and rotation axes, as illustrated in Fig. 1.

In the Crab pulsar, the phase spacing of the high-energy pulses is 0.4 of a period. Combining this with the evidence, gathered from the nature of the pulsed radio emission (see Kirk et al. 2002), that the observer passes almost directly over the magnetic pole, fixes both to be roughly 60° . This

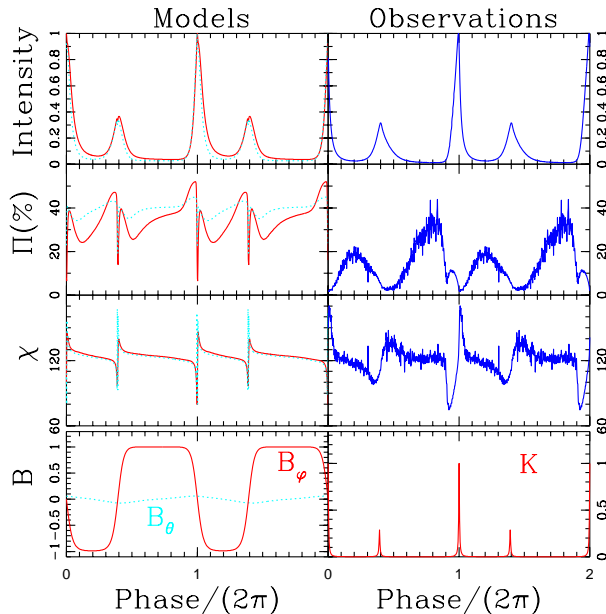


Fig. 2.— Model light curves of the intensity, degree of polarisation and position angle of the pulsed synchrotron emission compared to measurements of the Crab pulsar (Kellner 2002; Kanbach et al. 2003) (from Pétri & Kirk (2005)). Models with Lorentz factor $\Gamma = 20$ (solid line, red on-line) and 50 (dotted line, cyan on-line) are shown. The inclination of the line of sight equals the obliquity: $\alpha = \zeta = 60^\circ$ and the position angle of the projection of the pulsar’s rotation axis was set to 124° (Ng & Romani 2004). The bottom panels show the dependence on phase of the modelled magnetic field and particle density in the comoving frame.

agrees with an independent determination of $\zeta = 61.3 \pm 0.1$ from the morphology of the X-ray torus (Ng & Romani 2004).

High time-resolution polarimetry of the Crab pulsar (Kellner 2002; Kanbach et al. 2003) places additional, independent constraints on this model. The high-energy pulsed emission (optical to gamma-ray) originates as the synchrotron radiation of relativistic particles accelerated primarily in the current sheets. The magnetic field reverses direction across a sheet, but, in reality, this must occur over a region of finite width. Within such a region, the density of hot particles will rise, but the magnetic field intensity should decrease. It may become turbulent, and, instead of a pure neutral sheet, any residual poloidal field

component could cause a sweep of the field direction rather than a discontinuous jump. To some extent, the population of heated particles must also leak into the stripes surrounding the sheet, in which case, the toroidal magnetic field component should dominate and manifest itself in the polarisation direction. These effects have recently been modelled (Pétri & Kirk 2005) and compared to the data. The results, displayed in Fig. 2 show that it is possible to obtain reasonably good agreement for the intensity and degree of polarisation. For the angle of polarisation, very good agreement is achieved with the observed sense and size of the polarisation sweeps through the pulses. Particularly noteworthy, however, is the excellent agreement between the observed orientation of the linear polarisation vector between the pulses and the predicted orientation. Within the model, this is not sensitive to the choice of parameters, being coincident with the projection of the rotation axis of the pulsar on the sky. This is determined independently of the polarisation observations from measurements of the X-ray morphology of the nebula (Ng & Romani 2004).

Thus, the “smoking gun” of magnetic energy dissipation in pulsar winds may already have been detected (see Arons 2004). However, much work will be needed to develop particle acceleration models in these sheets before it becomes possible to estimate the calibre of the “gun”, where it fires, and how the trigger mechanism works.

3. High-energy emission from PSR 1259-63

The prospect of additional observational constraints on the structure of a pulsar wind has been opened up by the recent detection of high-energy (TeV) gamma-rays from the Be-star/pulsar binary system PSR 1259-63 by the H.E.S.S. array of imaging Čerenkov telescopes (Schlenker et al. 2005; Aharonian, F., et al., HESS Collaboration 2005). This binary comprises a pulsar of period 48 ms in an eccentric, 3.4 year orbit about a luminous Be star. Both stars presumably drive off winds, which interact, producing X-rays (Tavani

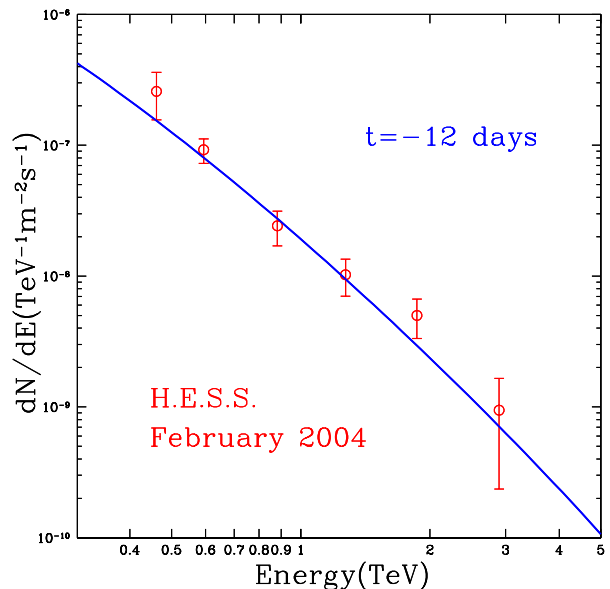


Fig. 3.— Predicted spectrum of inverse Compton scattered photons from the shocked pulsar wind plasma in the binary system PSR 1259-63, 12 days prior to periastron (Kirk et al. 1999), and the spectrum observed by the H.E.S.S. array of imaging Čerenkov detectors in February 2004 (Schlenker et al. 2005; Aharonian, F., et al., HESS Collaboration 2005)

& Arons 1997). Furthermore, both winds originate on rapidly rotating objects and are thought to have strong pole to equator variations. Modelling of the unpulsed radio emission suggests that the axis of rotation of the Be star is not aligned with that of the binary (Ball et al. 1999), which complicates the dependence of the interaction on orbital phase. Relativistic electrons from the shocked pulsar wind are thought to be responsible for the X-rays, in which case they must also upscatter UV photons from the Be star to TeV energies. Modelling of this process led to the prediction shown in Fig. 3 for the multi-wavelength spectrum. The details of the flow pattern of the emitting plasma are unknown, so that it cannot be decided a priori, whether the radiating electrons suffer predominantly radiative or adiabatic losses. However, provided the electron spectrum can be “calibrated” using the synchrotron X-rays, this does not greatly influence the predicted TeV flux. The

relative intensities of the synchrotron and inverse Compton components, on the other hand, depend sensitively on the magnetic field strength in the source. Fig. 3 shows the predicted flux for a magnetic field of 0.3 G, as indicated by models of the unpulsed radio emission (Ball et al. 1999), and in agreement with estimates from the spin-down rate of the pulsar. The remarkable agreement in both spectrum and normalisation indicates not only that the emission mechanism was probably identified correctly, but also that the X-ray intensity and magnetic field strength vary little from one periastron passage to another.

In addition to the spectrum, the H.E.S.S. observations also revealed substantial fluctuations in the light curve of this system on a timescale of one day. These cannot be accounted for within a model such as that of Kirk et al. (1999), which assumes spherically symmetric stellar winds. However, fluctuations are certainly to be expected if either or both winds is asymmetric about the normal to the plane of the orbit, especially close to periastron, where the true anomaly varies rapidly. A correlation with the unpulsed radio flux (Johnston et al. 2005) would be important in this connection, possibly indicating a connection with the passage of the pulsar through the equatorial outflow zone of the Be star (Kawachi et al. 2004).

The model underlying the prediction in Fig. 3 assumes the Lorentz factor of the pulsar wind just before it enters the termination shock located between the two stars is a few times 10^7 . At periastron, this point is, at most, a few thousand light cylinder radii from the pulsar, and can grow to a few hundred thousand at apastron — minute compared to the $10^9 r_L$ stand-off distance of the termination shock of the Crab pulsar. At first sight, therefore, the relatively high Lorentz factor appears to favour more rapid conversion of magnetic energy to particle energy than could be accommodated in the gradual acceleration models of Kirk & Skjæraasen (2003). But the extent to which it will be possible to test pulsar wind acceleration theories, for example by placing firm limitations

on the radial variation of the Lorentz factor, will depend on the availability of simultaneous X-ray and hard gamma-ray observations throughout the orbit, as well as the development of more sophisticated spectral modelling techniques.

I thank J. Arons, J. Pètri and Y. Lyubarsky for helpful discussions. This research was supported in part by the National Science Foundation under Grant No. PHY99-0794 and by a grant from the G.I.F., the German-Israeli Foundation for Scientific Research and Development.

REFERENCES

- Aharonian, F., et al., HESS Collaboration. 2005, A&A in press
- Arons, J. 2004, in *Young Neutron Stars and their Environments*, IAU Symposium #218, 163
- Ball, L., Melatos, A., Johnston, S., & Skjæraasen, O. 1999, *ApJ*, 514, L39
- Begelman, M. C. 1998, *ApJ*, 493, 291
- Bogovalov, S. V. 2001, *A&A*, 371, 1155
- Bogovalov, S. V., Chechetkin, V. M., Koldoba, A. V., & Ustyugova, G. V. 2005, *MNRAS*, 358, 705
- Coroniti, F. V. 1990, *ApJ*, 349, 538
- Daugherty, J. K., & Harding, A. K. 1982, *ApJ*, 252, 337
- Del Zanna, L., Amato, E., & Bucciantini, N. 2004, *A&A*, 421, 1063
- Gaensler, B. M., Arons, J., Kaspi, V. M., Pivovarovoff, M. J., Kawai, N., & Tamura, K. 2002, *ApJ*, 569, 878
- Gaensler, B. M., Pivovarovoff, M. J., & Garmire, G. P. 2001, *ApJ*, 556, L107
- Gaensler, B. M., Schulz, N. S., Kaspi, V. M., Pivovarovoff, M. J., & Becker, W. E. 2003, *ApJ*, 588, 441

- Helfand, D. J., Gotthelf, E. V., & Halpern, J. P. 2001, *ApJ*, 556, 380
- Hester, J. J., Mori, K., Burrows, D., Gallagher, J. S., Graham, J. R., Halverson, M., Kader, A., Michel, F. C., & Scowen, P. 2002, *ApJ*, 577, L49
- Hester, J. J., Scowen, P. A., Sankrit, R., Burrows, C. J., Gallagher, J. S., Holtzman, J. A., Watson, A., Trauger, J. T., Ballester, G. E., Casertano, S., Clarke, J. T., Crisp, D., Evans, R. W., Griffiths, R. E., Hoessel, J. G., Krist, J., Lynds, R., Mould, J. R., O’Neil, E. J., Stapelfeldt, K. R., & Westphal, J. A. 1995, *ApJ*, 448, 240
- Hirschman, J. A., & Arons, J. 2001a, *ApJ*, 554, 624
- . 2001b, *ApJ*, 560, 871
- Johnston, S., Ball, L., Wang, N., & Manchester, R. N. 2005, *MNRAS*, 358, 1069
- Kanbach, G., Kellner, S., Schrey, F. Z., Steinle, H., Straubmeier, C., & Spruit, H. C. 2003, in *Instrument Design and Performance for Optical/Infrared Ground-based Telescopes*. Edited by Iye, Masanori; Moorwood, Alan F. M. *Proceedings of the SPIE*, Volume 4841, pp. 82-93 (2003), 82–93
- Kawachi, A., Naito, T., Patterson, J. R., Edwards, P. G., Asahara, A., Bicknell, G. V., Clay, R. W., Enomoto, R., Gunji, S., Hara, S., Hara, T., Hattori, T., Hayashi, S., Hayashi, S., Itoh, C., Kabuki, S., Kajino, F., Katagiri, H., Kifune, T., Ksenofontov, L., Kubo, H., Kushida, J., Matsubara, Y., Mizumoto, Y., Mori, M., Moro, H., Muraishi, H., Muraki, Y., Nakase, T., Nishida, D., Nishijima, K., Ohishi, M., Okumura, K., Protheroe, R. J., Sakurazawa, K., Swaby, D. L., Tanimori, T., Tokanai, F., Tsuchiya, K., Tsunoo, H., Uchida, T., Watanabe, A., Watanabe, S., Yanagita, S., Yoshida, T., & Yoshikoshi, T. 2004, *ApJ*, 607, 949
- Kellner, S. 2002, Master’s thesis, Technische Universität München
- Kennel, C. F., & Coroniti, F. V. 1984, *ApJ*, 283, 710
- Kirk, J. G., Ball, L., & Skjæraasen, O. 1999, *Astroparticle Physics*, 10, 31
- Kirk, J. G., & Skjæraasen, O. 2003, *ApJ*, 591, 366
- Kirk, J. G., Skjæraasen, O., & Gallant, Y. A. 2002, *A&A*, 388, L29
- Komissarov, S. S., & Lyubarsky, Y. E. 2003, *MNRAS*, 344, L93
- . 2004, *MNRAS*, 349, 779
- Lu, F. J., Wang, Q. D., Aschenbach, B., Durouchoux, P., & Song, L. M. 2002, *ApJ*, 568, L49
- Lyubarsky, Y., & Kirk, J. G. 2001, *ApJ*, 547, 437
- Lyubarsky, Y. E. 2003, *MNRAS*, 345, 153
- Michel, F. C. 1994, *ApJ*, 431, 397
- Mori, K., Burrows, D. N., Hester, J. J., Pavlov, G. G., Shibata, S., & Tsunemi, H. 2004, *ApJ*, 609, 186
- Ng, C.-Y., & Romani, R. W. 2004, *ApJ*, 601, 479
- Pavlov, G. G., Teter, M. A., Kargaltsev, O., & Sanwal, D. 2003, *ApJ*, 591, 1157
- Pétri, J., & Kirk, J. G. 2005, *ApJ*, 000, in press
- Schlenker, S., Beilicke, M., Khelifi, B., Master-son, C., de Naurois, M., Rolland, L., & Hess Collaboration. 2005, in *AIP Conf. Proc. 745: High Energy Gamma-Ray Astronomy*, 341–346
- Shibata, S., Tomatsuri, H., Shimanuki, M., Saito, K., & Mori, K. 2003, *MNRAS*, 346, 841
- Spitkovsky, A., & Arons, J. 2004, *ApJ*, 603, 669
- Tavani, M., & Arons, J. 1997, *ApJ*, 477, 439

Vlahakis, N. 2004, ApJ, 600, 324

Weisskopf, M. C., Hester, J. J., Tennant, A. F.,
Elsner, R. F., Schulz, N. S., Marshall, H. L.,
Karovska, M., Nichols, J. S., Swartz, D. A.,
Kolodziejczak, J. J., & O'Dell, S. L. 2000,
ApJ, 536, L81